Electronic properties of tubule forms of hexagonal BC_3

Yoshiyuki Miyamoto,* Angel Rubio,† Steven G. Louie, and Marvin L. Cohen
Department of Physics, University of California at Berkeley, Berkeley, California 94720
and Materials Sciences Division, Lawrence Berkeley Laboratory, Berkeley, California 94720
(Received 27 July 1994; revised manuscript received 13 September 1994)

First-principles and tight-binding electronic-structure calculations of hypothetical tubule forms of hexagonal BC_3 have been performed. According to the total-energy and force calculations, stable atomic geometries of the BC_3 tubules can be obtained by rolling hexagonal BC_3 sheets keeping the C—C and C—B lengths at 1.42 and 1.55 Å, respectively. Since the energy increase upon tubule formation is smaller than that of carbon tubules, we conclude that the BC_3 tubules are likely to form. The planar BC_3 sheet has π and π^* bands above the Fermi level, and this feature is retained in the electronic structures of the BC_3 tubules. The influence of concentric formations of the BC_3 tubules on their conductivities is also discussed.

I. INTRODUCTION

The discovery of carbon-based tubules[1] has opened opportunities for obtaining material systems with nanoscale structures. Recently, classes of tubules originating from hexagonal compounds, i.e., BN and BC_2N, have been proposed.[2,3] The geometric and electronic properties of these tubules have been predicted theoretically leading to possibilities for technological applications. Either semiconducting or metallic behavior is predicted for carbon tubules depending on their radii and chiralities,[4,5] while BN tubules have an almost constant band gap (E_g) of 5.5 eV independent of their structures according to a recent first-principles quasiparticle calculation.[6] The BN tubules have free-electron-like states at the bottom of the conduction bands. These states have a maximum wavefunction amplitude in the inner region of the tubules. High conductivity is therefore expected for donor doping of these systems. On the other hand, predictions for chiral BC_2N tubules[3] raise the possibility that they behave as nanoscale coils because of the anisotropic conductivity of the original sheets. This is in contrast to the more isotropic carbon and BN tubules.

Previous total-energy calculations[3,6] also imply that the hexagonal compound sheets are as likely to form tubules as the graphite sheets. Indeed, tubule forms of the hexagonal compounds of B, C, and N have been recently observed experimentally in an arch-discharge setup.[7] Using chemical analysis, it has been determined that part of the samples have an atomic composition of B:C $\simeq$ 1:3. This result suggests the existence of BC_3 tubules and theoretical study is required to clarify the stability and the electronic properties of these tubules.

In this paper, we show that the relative stability of BC_3 tubules is comparable to that of carbon tubules and that their electronic structures can be well understood from the folding of a flat BC_3 sheet in the same manner as for the case of the carbon tubules.[4,5] Contrary to carbon, BN, and BC_2N sheets, a BC_3 sheet has both the π and π^* bands above the Fermi level (E_F),[8] which were observed by electron-energy-loss spectroscopy (EELS).[9] We found these main features of the electronic structure remain in the tubule forms so that the BC_3 tubules are expected to be distinguishable from the carbon tubules and the N-containing compound tubules by EELS measurement.

A single sheet of hexagonal BC_3 has semiconducting properties, and it becomes metallic when formed in multiple layers.[8] The metallic behavior is a result of the dispersion induced by interlayer interactions of the unoccupied π^* band to be below the occupied states. In a recent experiment in which these tubules are observed,[7] coaxially multiwall arrangement structures are observed similar to carbon tubules. Hence the electronic structure of concentric tubules will be influenced by interwall interactions, which would be of the same order as the interlayer interactions in layered BC_3 sheets.

This paper is organized as follows. In Sec. II we briefly describe the method for the calculations. In Sec. III A, we discuss the atomic geometry of the hexagonal BC_3 sheet and present results of the band structures for a single sheet obtained using local-density-approximation (LDA) and tight-binding (TB) schemes. In Sec. III B, we describe how to obtain tubule forms from BC_3 sheets and present strain energies and band structures for single-wall BC_3 tubules. In Sec. III C, we consider the influence of layer-layer interactions on the multiple BC_3 sheets on their electronic structures and discuss the case of concentric BC_3 tubules. Finally, we briefly summarize our results.

II. CALCULATION

The present first-principles calculations are carried out within the LDA. We use a plane-wave basis set with a cutoff energy of 36 Ry and use *ab initio* pseudopotentials obtained with the Kleinman-Bylander scheme.[10] In the calculation of a single BC_3 sheet, we use three-dimensional periodic boundary conditions with repeated sheets at a distance of 7.7 Å. For the calculations of the BC_3 tubules,

we again use three-dimensional periodic boundary conditions assuming that the tubules are aligned in a hexagonal unit cell. In this geometry the closest distance between atoms at adjacent tubules is set at 4.8 Å. This distance has been found to be far enough to avoid interactions between neighboring tubules. Hellmann-Feynman forces on each atom of the BC_3 sheets and of the tubules are calculated to evaluate the stability.

For the TB calculation, the nearest-neighbor interaction parameters for s, p, and s^* basis orbitals[11] are determined so that these parameters reproduce the LDA results in an energy region near E_F for a single sheet of hexagonal BC_3. We use these TB parameters for the band-structure calculations of a variety of tubule structures.

III. RESULTS

A. BC_3 single sheet

A possible structure for hexagonal BC_3 was proposed in an experimental study.[12] The structure is shown in Fig. 1 in which B–B bonds are excluded because these bonds are less stable than C–C and C–B bonds. An LDA calculation of this geometry was carried out using a localized basis sets. Bond lengths of $d_{C-C} = 1.42$ Å and d_{C-B}=1.55 Å were found to minimize the total energy of the system.[8] In the present calculation using a plane-wave basis set, these bond lengths are found to generate atomic forces less than 0.01 Ry/a.u. on each atom. Figure 2(a) shows our results for the band structure of a single BC_3 sheet which agrees well with previous results[8] except for the free-electron-like conduction bands located 4.5 eV above E_F at the Γ point. (The existence of free-electron-like bands above E_F is systematically seen in the BN and BC_2N sheets and tubules,[3,6] which cannot be described well with limited localized basis sets.) The top of the valence bands has σ character while the bottoms of the first and second conduction bands have π and π^* characters, respectively. The monolayer has a small indirect E_g (~0.5 eV) which would disappear in the multilayer form (the results of multilayers will be discussed in Sec. III C). Figure 2(b) shows an sp^3s^* TB result of the BC_3 sheet which agrees with the LDA result in an energy region near E_F. This agreement suggests that it is appropriate to use the sp^3s^* TB parameters for the electronic structure of other more complex BC_3 tubules (see the next section).

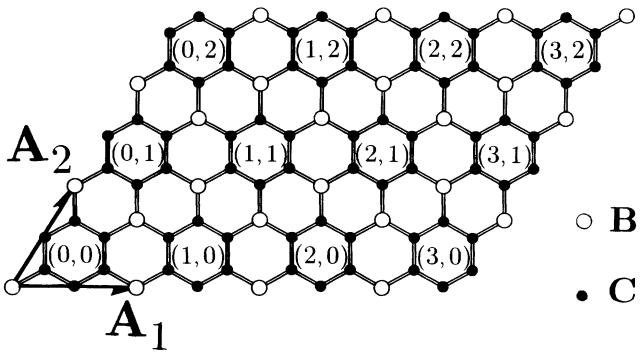

FIG. 1. Proposed structure for hexagonal BC_3. Large open circles and small solid circles denote B and C atoms, respectively. $\mathbf{A}_1$ and $\mathbf{A}_2$ are lattice vectors of the unit cell. Lattice indices are shown on each unit cell indicating the different ways of rolling this sheet into tubules.

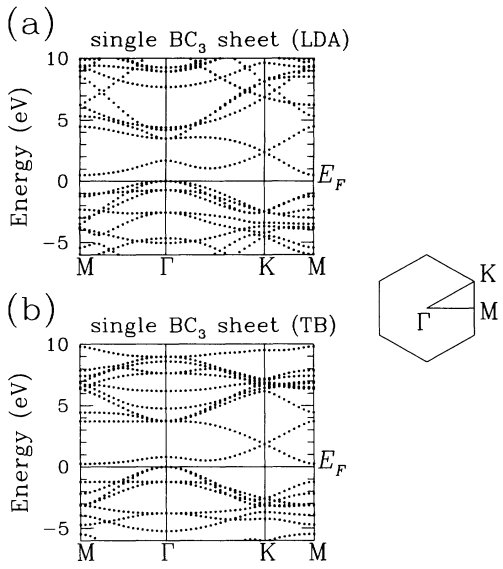

FIG. 2. Band structure of a single BC_3 sheet obtained by (a) LDA and (b) TB calculations. The Brillouin zone is also shown.

B. BC_3 tubules

The structures of the BC_3 tubules can be classified by the notation (n, m) in analogy with carbon tubules:[4,5] The (n, m) tubule of BC_3 is obtained by rolling the sheet so that the unit cell at the position (0,0) in Fig. 1 connects to another unit cell at the position (n, m). Hereafter we denote the (n, m) tubule of BC_3 as the BC_3 (n, m) tubule. Since the unit cell of BC_3 is about four times larger than that of the graphite, the sizes of the BC_3 (n, m) tubules are comparable to those of the $(2n, 2m)$ carbon tubules. In the LDA and TB calculations, we assume that the atomic coordinates of the (n, m) tubules are directly obtained by rolling the sheet keeping the bond lengths the same as those in the sheet.

The LDA total-energy and force calculations have been done on BC_3 (3,0), (4,0), and (2,2) tubules. According to our calculation, forces on each atom in the BC_3 tubules are very small, comparable to those of the flat sheet. This fact indicates that the present geometrical assumptions are accurate enough to determine the atomic geometries for BC_3 tubules. Strain energies of the BC_3 tubules have been obtained by comparing the calculated total energies of tubules with that of the planner sheet. Figure 3 shows the strain energies of carbon and BC_3 tubules which are fitted with a classic elastic function proportional to $\frac{1}{D^2}$. Here, D is a diameter of the tubule, and one notes that

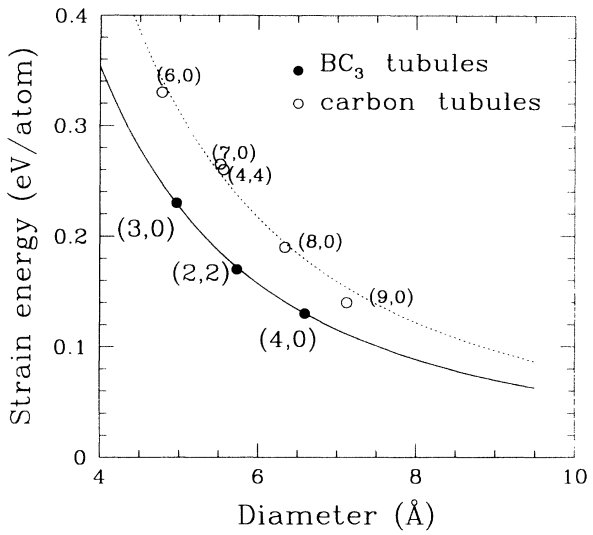

FIG. 3. Strain energies of the carbon tubules (open circles and the dotted line) and the BC_3 (n,m) tubules (solid circles and the solid line) upon rolling the planar sheet obtained by LDA calculations. The data points are fitted to a function proportional to $\frac{1}{D^2}$. Here D is a diameter of the tubule. Corresponding indices (n,m) for carbon and BC_3 tubules are also indicated with small and large letters, respectively.

the strain energies of the BC_3 tubules are smaller than those of the carbon tubules. The strain energies of the BC_3 tubules are found to be comparable to those of the BN tubules.[6] We therefore expect that the BC_3 tubules are likely to form as well as the carbon and BN tubules.

Figure 4 shows band structures for the BC_3 (2,2) tubule, obtained by LDA calculations and by sp^3s^* TB calculations. The general features of the band structure agree well when comparing LDA and TB calculations. In both cases (Fig. 4), one can see that there are two particular conduction bands which cross each other at a k vector of exactly (a little farther than) two-thirds of the way from the Γ point to the X point in the Brillouin zone for the TB (LDA) result. These bands have π- and π^*-bonding characters. Other conduction bands above E_F also have the same character. These features can be derived by computing the π- and π^*-band dispersions along one-dimensional k-vector lines in momentum space for the hexagonal BC_3, in a similar manner as for the case of carbon tubules:[4,5] The tubule π and π^* bands correspond to those of the sheet running from the Γ to K points, from the M to K points, and from an intermediate point between the Γ and M points to another M point in the Brillouin zone of the hexagonal BC_3. (The crossing point of the tubule π and π^* bands corresponds to the K points of the hexagonal BC_3.) Based on this agreement for the TB and LDA results for the small BC_3 (2,2) tubule (radius=2.84 Å) we can assume that the TB results will describe well the electronic structure of large tubules, for which the LDA calculation becomes expensive and time consuming because of the large unit cell. Indeed, we have found that the crossing points of π and π^* bands for the LDA and TB results become closer to each other for the case of the BC_3 (4,4) tubule which is not shown here.

The band structures of the (n,n) (n=3,4,5) tubules have been obtained by the TB calculation, see Fig. 5. The carbon (n,n) single-wall tubules behave like metals, while the BC_3 (n,n) single-wall tubules are semi-

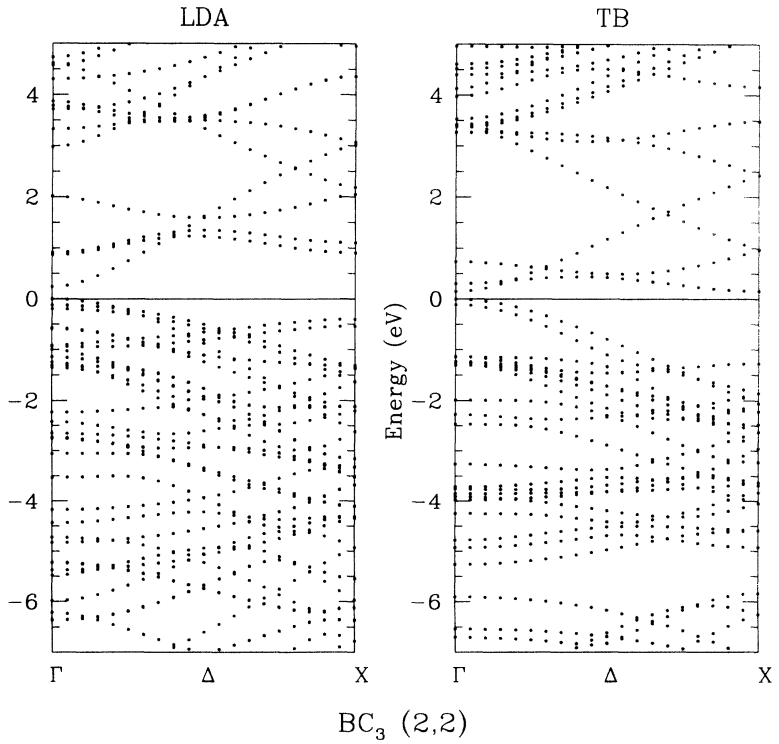

FIG. 4. Band structures of the BC_3 (2,2) tubule calculated using the LDA (left panel) and sp^3s^* TB (right panel). The locations of E_F are denoted by solid horizontal lines.

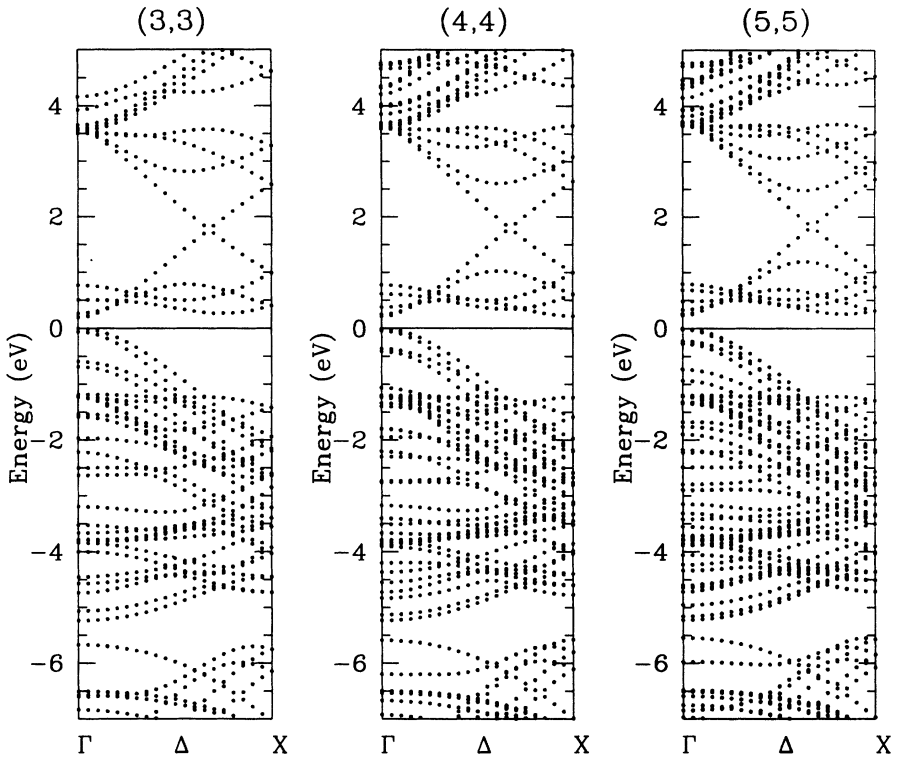

FIG. 5. Band structures of the BC_3 (n,n) $(n$=3,4,5) tubules obtained by sp^3s^* TB calculations. The E_F corresponds to 0 eV.

conducting. The location of E_F is between the π and σ bands which is the same as the BC_3 sheet resulting in semiconducting behavior for the tubules. The calculated E_g (~0.2 eV) of the (n,n) $(n$=3,4,5) tubules is close to that of the BC_3 sheet obtained in the TB calculations as shown in Fig. 2(b).

We have also calculated the band structures of the $(n,0)$ tubules by using the TB scheme; these are shown in Fig. 6. In this case, the band structures can also be understood from the folding of the bands of the single sheet. We note that there are two conduction bands close to each other at the Γ point located at about 1.7

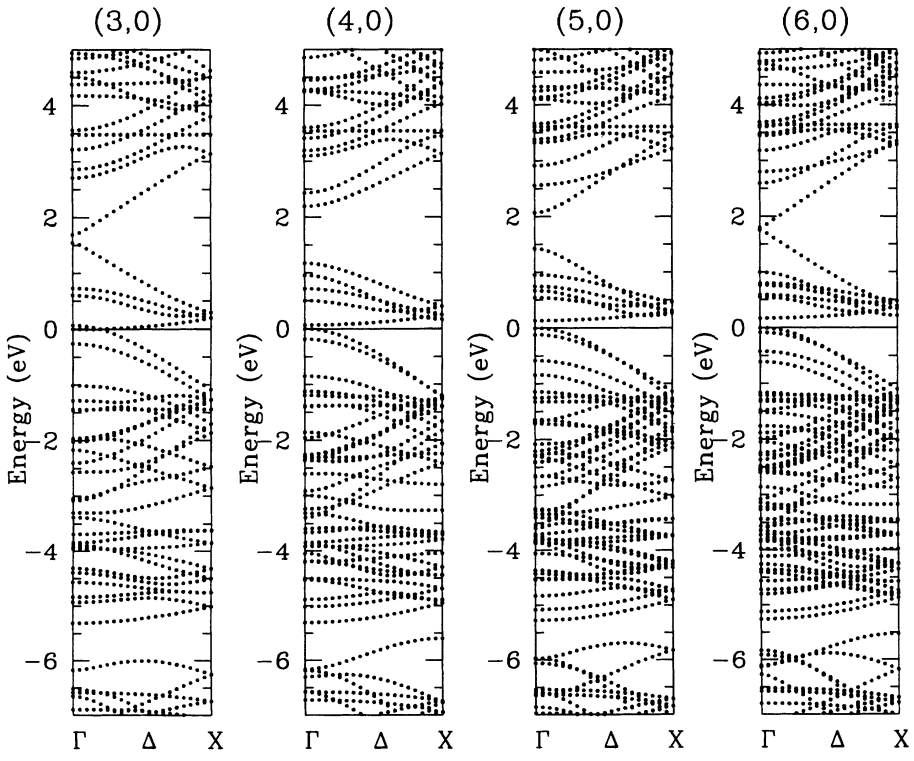

FIG. 6. Band structures of BC_3 $(n,0)$ $(n$=3–6) tubules obtained by sp^3s^* TB calculations. The E_F corresponds to 0 eV.

eV above E_F for the cases of n=3 and 6. For these structures the tubule k vector coincides with the K point of the original BC_3 sheet when $n = 3 \times m$, where m is an integer. This feature corresponds to the E_g oscillation in the carbon $(n,0)$ tubules.[4,5] However, E_F here is lower than the π bands and the BC_3 $(n,0)$ tubule E_g's do not show the oscillation.

The TB results do not give the oscillation but rather a metal-semiconductor transition for the BC_3 $(n,0)$ tubules with increasing diameter. (We note that we have underestimated E_g because the TB parameters were obtained from the LDA results. Hence we expect that for a quasiparticle band-structure calculation instead of a metal-semiconductor transition, there will be a variation of increasing E_g for the semiconducting single-wall tubules.) This trend may be understood from a change in the bond angles of the atoms. With a finite diameter, the curvature of the wall makes the bond angles less than the sp^2 ideal angle of 120° resulting in an intermediate orbital hybridization for the σ bonds which now have an admixture of the sp^3 hybridization. The σ states therefore contain an excess p-orbital component compared to those of the flat sheet, which gives rise to an increase in their energy. On the other hand, the π states now contain an excess s-orbital component which lowers their energy. Hence the E_g's of the $(n,0)$ BC_3 tubules are decreased in the cases of small tubule diameters and the E_g converges to that of the flat sheet in an infinite-diameter limit. Contrary to the $(n,0)$ tubules, the (n,n) tubules have an almost constant E_g independent of their diameters. This difference in behavior results from of the geometrical difference between the $(n,0)$ and (n,n) tubules. Table I lists the averaged bond angles for (n,n) and $(n,0)$ tubules. A more rapid convergence to 120° for the back bond angle is seen for the (n,n) tubules with larger index n compared to the case of $(n,0)$ tubules. The E_g's of the (n,n) tubules therefore appear to converge to that of the flat sheet quicker as a function of n.

Figure 7 shows the results for the density of states (DOS's) of a single BC_3 sheet and a (2,2) tubule obtained by LDA calculations. The two sharp peaks above E_F originating from the π and π^* bands are seen in both systems indicating that an EELS measurement of the BC_3 tubules would give similar results as observed for the BC_3 sheets.[9] The lower of the two peaks could be below E_F in the DOS of the BN and BC_2N tubules as well as carbon tubules. So we expect that the appearance of these two peaks can be used as evidence for the existence

TABLE I. Averaged bond angles θ and diameters D of the BC_3 $(n,0)$ and (n,n) tubules. Atomic coordinates are generated assuming that C–C and C–B bond lengths are kept at 1.42 Å and 1.55 Å, respectively, upon rolling BC_3 sheets into tubules.

Tubule	θ (degree)	D (Å)	Tubule	θ (degree)	D (Å)
(2,2)	118.3	5.74	(3,0)	117.8	4.97
(3,3)	119.3	8.55	(4,0)	118.8	6.59
(4,4)	119.6	11.38	(5,0)	119.1	8.22
(5,5)	119.7	14.21	(6,0)	119.4	9.85

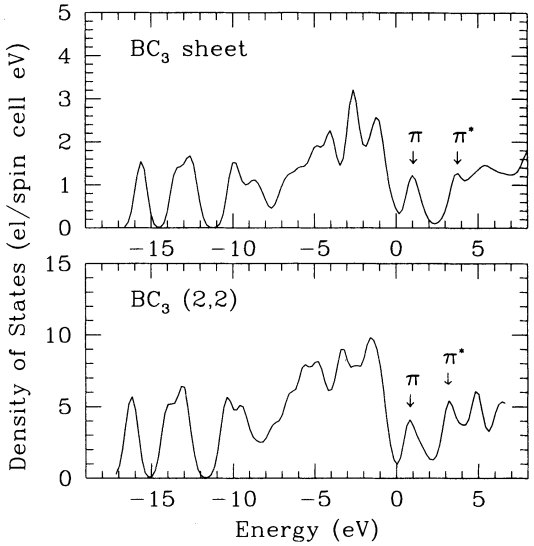

FIG. 7. Density of states of a single BC_3 sheet (upper panel) and the (2,2) tubule (lower panel) obtained from LDA calculations. In each case, E_F corresponds to 0 eV. Peaks derived from conduction π and π^* bands are indicated by arrows.

of the BC_3 tubules. We note here that the same features should be observed in the EELS of multiply stacked BC_3 layers making this feature of EELS characteristic of the BC_3 compounds.

Here, we propose a possible way of doping the single-wall BC_3 tubules with hole carriers which would make the σ bands metallic. In the cases of the carbon tubules, the substitution of C atoms with B atoms may induce hole carriers in the tubules. On the other hand, substituting a C atom with a B atom in the BC_3 tubules would inevitably introduce a B–B bond, which was excluded from consideration in previous studies[8,12] and has recently been found to be energetically unfavorable.[13] Instead of excess B atoms, we expect that the introduction of halogen atoms could induce hole carriers on the tubules due to the halogen's large electronegativities. In the graphite intercalation compounds,[14] some halogens, (i.e., Cl, Br, and I) behave as acceptors. If a similar phenomenon occurs for BC_3 tubules, the introduction of halogen atoms induced by capillarity effects[15] would lower the tubule E_F resulting in conductivity from the σ bands which is expected to be larger than the one in carbon tubules where the conductivity is based on the π bands.

C. Multiple sheets and concentric tubules of BC_3

In previous calculations,[8] metallic behavior for multiple BC_3 sheets was found. Two types of sheet stacking were considered, i.e., AA and AB stacking forms, with the sheet-sheet distance at 3.35 Å determined from the experimental value.[12] In both the AA- and AB-stacking forms, each atom on one sheet is located directly above another one on the neighboring sheet below. In the AA

stacking form all atoms sit above atoms of the same kind, while in the AB stacking form all B atoms sit above C atoms. We present here details of the band structures for these stacking forms (which were not shown in previous calculations[8]) in order to describe the influence of the interlayer interaction on the details of the band structures. Figures 8(a) and 8(b) show band structures of the AA- and AB-stacking forms obtained by our present LDA calculations. One can distinguish the σ and π character of each band by considering the dispersion in the k_z direction, i.e., the normal direction to the sheet which corresponds to the direction from M to L points in Fig. 8. In the k_z direction, the π bands have considerable dispersion while the σ bands have almost no dispersion. In the AA stacking form, the conduction π^* band goes below the top of the σ bands in the direction from the M to L point resulting in a lowering of E_F. The σ band becomes a fractionally occupied band and dominates the conductivity of the system. On the other hand, in the AB stacking form, the π^* band is below E_F in the K–M and M–L directions, but here it is hard to conclude that the σ bands are responsible for most of the metallic behavior. We have also calculated the DOS of each stacking form, which are not shown here. The DOS at E_F of the AB stacking form has been found to be lower than that of the AA stacking form, which agrees with the previous results.[8] A lower total energy is then expected for the AB stacking form but the calculated energy difference is very small because of unreliability of LDA in estimating the van der Waals-type interlayer interactions. In any case, the AB stacking form seems to be dominant experimentally.

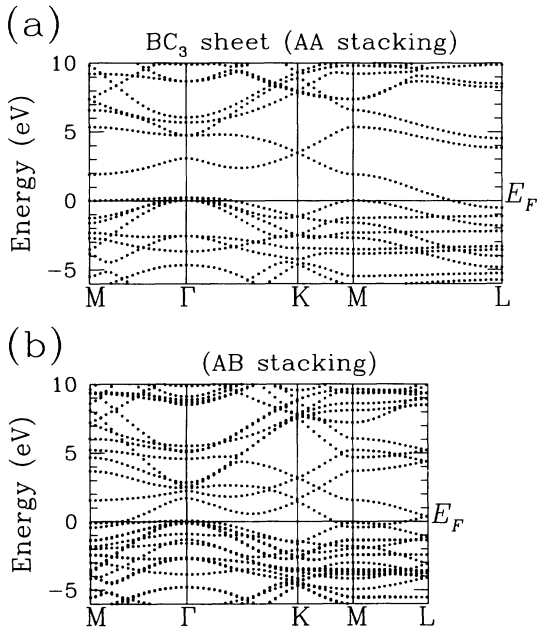

FIG. 8. Band structure of (a) AA and (b) AB stacking forms of BC_3 multiple sheets obtained by LDA calculations. The Brillouin zone of the AB stacking form is half of that of the AA stacking form. The AB stacking form has two inequivalent M points in the Brillouin zone, one of which is not shown here.

We next consider the electronic structures of concentric BC_3 tubules. We expect from calculations for multiple sheets that the interwall interaction of the concentric tubules will make the conduction band overlap the valence-band maximum similar to the case of the multiple sheets. If this occurs, the tubule σ bands would cross E_F and then the tubules will have conducting walls. This can be regarded as wall-wall induced conductivity in the tubule axis direction. By analogy with multiple flat sheets, conductivity originating from the σ band could be dominant in a concentric needle of BC_3 tubules. (If so, this is a new phenomenon not seen in other types of tubules studied previously.) For the concentric tubules, a reasonable wall-wall distance would be of the same order as the sheet-sheet distance of 3.35 Å since the origin of the cohesion of the concentric tubules is likely of the van der Waals-type interaction. For the tubules of either carbon or BN, a pair of the (4,4) and (9,9) tubules, for example, yields a reasonable wall-wall distance.[6] On the other hand, the corresponding pair of the BC_3 tubules is the (2,2) and (4.5,4.5) tubules, with the later not possible from rolling the BC_3 sheet. The BC_3 (n,n) tubules are thus expected to not have concentric forms. We have found that every possible pair of the experimental wall-wall distance including chiral tubules is incommensurate. One open question here is how many walls are necessary to give rise to conductivity in concentric BC_3 tubules. That is equivalent to looking for the semiconductor-metal transition as a function of the number of the concentric shells of the tubules. Unfortunately, this question cannot be solved directly by conventional band-structure calculations at present because of the geometrical difficulty of the incommensurate phases. More theoretical formalisms would be helpful for attacking this interesting problem.

IV. CONCLUDING REMARKS

We have performed band-structure calculations on BC_3 sheets and tubules within the LDA and TB schemes. The main qualitative feature of the tubule band structures can be derived from those of BC_3 sheets in the same manner as in the case of carbon tubules.[4,5] According to LDA total-energy and force calculations for the BC_3 tubules, it is concluded that the BC_3 tubules are as likely to form as carbon and BN tubules. Atomic buckling was found to stabilize the BN tubules,[6] while the BC_3 tubules retain the graphitic sp^2 bonding on the wall. Contrary to the carbon, BN, and BC_2N tubules, the BC_3 tubules have both π and π^* bands above E_F so we expect that BC_3 tubules are distinguishable from the other tubules in EELS measurements. Concentric BC_3 tubules are expected to be metallic, but their electronic structures cannot be obtained by conventional band-structure calculations because of the incommensurate geometry of concentric BC_3 tubules.

ACKNOWLEDGMENTS

This work was supported by National Science Foundation Grant No. DMR91-20269 and by the Director Office

of Energy Research, Office of Basic Energy Sciences, Materials Sciences Division of the U.S. Department of Energy under Contact No. DE-AC03-76SF00098. Part of the present calculations were done using the CRAY-C90 computer at the San Diego Supercomputer Center and the CRAY-YMP computer at National Energy Research Supercomputer Center. We thank Professor A. Zettl, Professor R. Gronsky, and their co-workers for information about their experimental results prior to publication. Y.M. thanks Professor D. Rokhsar and Dr. C. Wang for comments on electronic structures of incommensurate phases, and acknowledges support from the Fundamental Research Laboratories of NEC Corporation. A.R. was supported by the Fullbright Commission.

---

* Permanent address: Fundamental Research Laboratories, NEC Corporation, 34 Miyukigaoka, Tsukuba 305, Japan.

† Permanent address: Departmento de Fisica Teórica, Universidad de Valladolid, E-47011 Valladolid, Spain.

[1] S. Iijima, Nature **354**, 56 (1991); S. Ijima and T. Ichihashi, *ibid.* **363**, 603 (1993).

[2] A. Rubio, J.L. Corkill, and M.L. Cohen, Phys. Rev. B **49**, 5081 (1994).

[3] Y. Miyamoto, A. Rubio, M.L. Cohen, and S.G. Louie, Phys. Rev. B **50**, 4976 (1994).

[4] R. Saito, M. Fujita, G. Dresselhaus, and M.S. Dresselhaus, Appl. Phys. Lett. **60**, 2240 (1992).

[5] N. Hamada, S. Sawada, and A. Oshiyama, Phys. Rev. Lett. **68**, 1579 (1992).

[6] X. Blase, A. Rubio, M.L. Cohen, and S.G. Louie, Europhys. Lett. (to be published).

[7] K. Cherrey *et al.* (unpublished).

[8] R.M. Wentzcovitch, M.L. Cohen, S.G. Louie, and D. Tománek, Solid State Commun. **67**, 515 (1988); D. Tománek, R.M. Wentzcovitch, S.G. Louie, and M.L. Cohen, Phys. Rev. B **37**, 3134 (1988).

[9] K.M. Krishnan, Appl. Phys. Lett. **58**, 1857 (1991).

[10] L. Kleinman and D.M. Bylander, Phys. Rev. Lett. **48**, 1425 (1982).

[11] P. Vogl, H.P. Hjalmarson, and J.D. Dow, J. Phys. Chem. Solids **44**, 365 (1983).

[12] J. Kouvetakis, R.B. Kaner, M.L. Sattler, and N. Bartlett, J. Chem Soc. Chem. Commun. 1758 (1986).

[13] R. Magri, Phys. Rev. B **49**, 2805 (1994).

[14] See, for example, M.S. Dresselhaus and G. Dresselhaus, Adv. Phys. **30**, 139 (1981), and references therein.

[15] P.M. Ajayan and S. Iijima, Nature **361**, 333 (1993).